

Deep water properties, velocities, and dynamics over ocean trenches

by Gregory C. Johnson¹

ABSTRACT

Observations of water properties and deep currents over several trenches in the Pacific Ocean central basins give consistent evidence for recent ventilation of water below the trench sills and cyclonic sense of circulation over the trenches. A dynamical argument for this pattern is advanced. First, a review of previous analyses of hydrographic data shows that the trenches are well ventilated by dense bottom water, that within the trenches this bottom water generally spreads away from its source, and that a cyclonic sense of circulation is suggested over some trenches. Then, this cyclonic sense of circulation over the trenches is further documented using deep current meter and float data. Finally, bathymetry is used to motivate a simple dynamical framework for flow over trenches. If the trench sides are sufficiently steep and the trench is sufficiently removed from the equator to ensure a region of closed geostrophic contours, then any upwelling over that region will drive a strong deep cyclonic recirculation in the weakly-stratified abyss through vortex stretching. The magnitude of this recirculation is limited by bottom drag. Ageostrophic flow in a bottom Ekman layer into the trench balances the water upwelled over the trench. The cyclonic recirculation is much stronger than the upwelling-driven flow predicted across blocked geostrophic contours by the linear planetary geostrophic balance.

1. Introduction

The classical theoretical framework for the thermohaline circulation of the abyssal ocean assumes localized sinking at high latitudes forced by buoyancy loss from air-sea exchange. This sinking is balanced by widespread upwelling at lower latitudes that in turn counters the effects of downward diffusion of buoyancy from the surface (Stommel and Arons, 1960). If upwelling increases with distance from the sea floor and bathymetry is sufficiently gentle to avoid regions of closed geostrophic contours, the planetary geostrophic balance dictates overall poleward interior flows. With a boundary condition of no net flow into the eastern edge of each basin, the interior flow is fed from deep western-boundary currents. These dynamics result in recirculation regions near the poles where interior flow feeds deep westward-flowing boundary currents at poleward walls. The deep western-boundary currents near these recirculations sometimes flow back toward the high latitude sources. Predictions of locations and strengths of deep boundary currents have

¹ Pacific Marine Environmental Laboratory, NOAA, 7600 Sand Point Way, N.E. (Bldg. 3), Seattle, Washington, 98115-0070, U.S.A.

been confirmed by observations in locations throughout the World Ocean (Warren, 1981). Many variations on this framework have been investigated, and a small sample are given below. Interior zonal jets have been observed and modeled flowing away from an eastern deep-water source (Warren, 1982) and toward an eastern deep-water sink (Warren and Speer, 1991; Speer *et al.*, 1995). The distortion of the circulation by gentle bathymetry has been discussed (Warren and Owens, 1985). Abyssal spin-up and nonuniform interior upwelling influences have been modeled (Kawase, 1987). Effects of a fully nonlinear continuity equation (Speer and McCartney, 1992) have also been investigated.

The focus of this work is abyssal circulation over deep trenches, specifically along the western and northern margins of the Pacific Ocean central basins. The simple Stommel-Arons framework must be modified substantially here because steep bathymetry results in regions of closed geostrophic contours over the trenches, a situation predisposed to strong recirculations (Welander, 1969). Theoretically, a dense bottom water source introduced into a stratified rotating deep basin shaped more like a bowl than a box can drive an anticyclonic interior circulation. This tendency, coined the hypsometric effect, results from decreasing vertical velocity with decreasing depth owing to the increasing area of the basin with decreasing depth (Rhines and MacCready, 1989). However, 1- $\frac{1}{2}$ and 2- $\frac{1}{2}$ layer numerical models as well as analytical results demonstrate that in situations where stratification is weak, upwelling over closed geostrophic contours is associated with a strong cyclonic recirculation tangent to the contours. The results are similar for elevated or depressed topography in sink-driven experiments with prescribed uniform upwelling (Straub and Rhines, 1990) and in source-driven basin-filling experiments (Kawase and Straub, 1991; Kawase, 1993a,b). The upwelling within the region of closed geostrophic contours results directly in vortex stretching that drives a strong cyclonic recirculation, limited only by bottom drag. A bottom Ekman layer associated with this drag transports mass into the region normal to the closed contours. If the circulation is in steady-state, the bottom Ekman transport balances the mass lost to upwelling within the region.

In the following, first a literature review shows several inferences about this deep flow from hydrographic data. Water properties below the trench sills reveal that bottom water there is not stagnant. That is to say, each series of trenches is actively ventilated by bottom water. In addition, water properties in some locations suggest flow patterns. In the Pacific, the inferences from the water properties are that the bottom water in these trenches is spread relatively rapidly away from its southern source and often that a cyclonic sense of circulation is evident. These two inferences are not contradictory since the southern bottom water signature can be carried rapidly away from its source on one branch of the cyclonic circulation around the trench. Next, velocity measurements are used to document a cyclonic sense of circulation over several trenches. Finally, the trench bathymetry is shown to result in closed geostrophic contours, and this fact is used to place the observations in a theoretical framework.

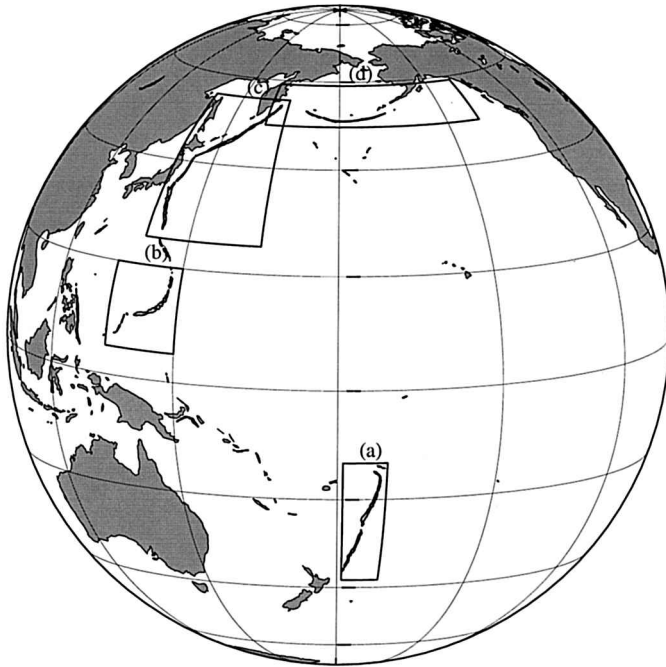


Figure 1. Deep trenches at the western and northern edges of the Pacific Ocean central basins revealed by the GEBCO 7000-m isobath (IOC, IHO, and BODC, 1994). The labeled boxed areas correspond to individual panels of Figure 5, and contain the trenches extensively discussed, (a) The Kermadec and Tonga Trenches, (b) the southern end of the Mariana Trench, (c) the Izu-Ogasawara, Japan, and Kuril Kamchatka Trenches, and (d) the Aleutian Trench.

2. Deep water properties

The Pacific Ocean is ringed around much of its margins by deep trenches (Fig. 1). Significant trenches are found elsewhere in the World Ocean. However, readily available long-term deep current measurements over trenches are all found at the western and northern edges of the Pacific Ocean central basins. For the sake of brevity, only water properties in this region will be discussed in detail. No bottom water forms in the North Pacific Ocean; instead it enters the Pacific Ocean central basins in a deep western-boundary current from the south. The following literature review starts closest to this bottom water source, with water properties of the Kermadec Trench, moves clockwise around the Pacific Ocean, and ends with the water properties of the Aleutian Trench, farthest from the source.

Zonal transpacific hydrographic sections at 32.5 and 28S (Whitworth *et al.*, 1996; Warren, 1973) cross the Kermadec Trench. The sections show that the water below the sill is about as cold (in potential temperature), fresh, dense, oxygen-rich, and silica-poor as bottom water just to the east. These properties are characteristics that distinguish the more recently ventilated modified Antarctic Bottom Water from the less recently ventilated

modified North Atlantic Deep Water. These water masses are the two main components of the Circumpolar Deep Water that ventilates the deep Pacific Ocean, with the former being dominant in the bottom water of the southern hemisphere, and the latter being dominant in the bottom water of the northern hemisphere. Properties below the trench sill distinguish water there as strongly southern in origin. This conclusion is not surprising, since the trench is coincident with the northward-flowing deep western-boundary current banked against the Kermadec Island Arc (Whitworth *et al.*, 1996; Warren, 1973). The oxygen-rich nature of the water below the sill clearly shows that water there is not stagnant. This water must be sufficiently ventilated to maintain this characteristic in the face of biological consumption. In addition, a trough in the isotherms immediately over the trench is visible to varying degrees in the four zonal sections near 32.5S and the single zonal section at 28S. Assuming geostrophy and a reference velocity of zero somewhat above the trough, this persistent feature is consistent with a bottom-intensified cyclonic sense of circulation over the trench, as noted by Whitworth *et al.* (1996).

Farther north, a zonal transpacific section across the north end of the Mariana Trench at 24N (Roemmich *et al.*, 1991) shows that the water below the trench sill is relatively cold, salty, dense, oxygen-rich, and silica-poor. A section near the saddle point of the Izu-Ogasawara and Japan Trenches at 35N (Kenyon, 1983) also shows these tendencies. In the North Pacific Ocean, these tendencies distinguish more newly arrived Circumpolar Deep Water below from the older Pacific Deep Water above. By this latitude the modified North Atlantic Deep Water component of Circumpolar Deep Water is dominant in the bottom water, which is why the distinguishing salinity and silica criteria for southern origin bottom water change from south to north. At both latitudes, water of more extreme southern characteristics is found offshore. However, the relatively oxygen-rich and silica-poor nature of water below the trench sills again argues for relatively recent ventilation with southern bottom water. Neither section has station spacing adequate to reveal near-bottom isotherm deflections over the trenches.

In zonal sections across the Kuril Kamchatka Trench at 42 and 47N, and a meridional section across the Aleutian Trench at 152W (Talley *et al.*, 1991), local water properties are most extreme in their southern characteristics below the trench sills. Data from four short meridional sections across the Aleutian Trench at 165E, 175E, and 175W, discussed previously following similar lines of inquiry (Warren and Owens, 1985; 1988), also support this hypothesis. The role of these trenches in spreading bottom water poleward along the western boundary and eastward along the northern boundary of the North Pacific Ocean has been discussed (Talley *et al.*, 1991; Talley and Joyce, 1992). A map of dissolved silica on a near-bottom potential isopycnal in the North Pacific Ocean (Talley and Joyce, 1992) clearly shows a tongue of silica-poor (and oxygen-rich) water. This tongue spreads poleward over the trench along the western boundary and then eastward over the equatorward side of the trench along the northern boundary. In addition, the northern and western boundary sections in this region show a narrow band of high silica at the boundary on the inshore side of the trench, implying southward and westward flow, respectively

(Warren and Owens, 1985; 1988; Talley *et al.*, 1991; Talley and Joyce, 1992). Finally, close examination of the seven individual sections across the trenches reported in these studies reveals slight troughs in isotherms directly over the trenches, again consistent with a bottom-intensified cyclonic sense of circulation over the trenches. However, with the weak shears and minimal water-property guidance in these abyssal regions, the inference of geostrophic flow direction from thermal wind is perilously dependent on the assumed reference velocities.

In summary, existing studies show that water below the sills of these trenches always has relatively, and sometimes extreme, southern water properties, suggesting that the trenches are well ventilated with bottom water of southern origin. Previous analysis of hydrographic data suggest decreasingly southern bottom water properties below the deep trench sills with increasing clockwise distance from the source in the southwest corner (progressing northward along the western boundary and then eastward along the northern boundary). Furthermore, evidence from the literature shows that the Kuril Kamchatka and Aleutian trenches rapidly spread bottom water away from the southern source. Studies detail how the deep silica distribution also suggests that there is a cyclonic sense of circulation over and within these trenches. Finally, published vertical sections show that deep isotherms just above the trenches are suggestive of a bottom-intensified cyclonic sense of circulation.

3. Deep velocities

Here data from six deep current meter arrays and one deep deployment of floats are discussed and shown to provide more evidence for a cyclonic sense of circulation over deep ocean trenches, greatly augmenting the information from water-property and density distributions. Most of these trenches are the same ones on the western and northern margins of the Pacific Ocean central basins discussed in the previous section. These measurements are reviewed working from south to north along the western boundary and then from west to east along the northern boundary, as before. Current directions here are reported as $^{\circ}\text{T}$, in degrees clockwise from north. For example, 90°T signifies eastward flow.

Recently, a current meter array was deployed across the Kermadec Trench at 32.5S to quantify the transport of the deep western-boundary current there. These data have been analyzed and discussed at some length (Whitworth *et al.*, 1996). A deep cyclonic sense of circulation is evident over the trench, superimposed on the equatorward flow of the deep western-boundary current. Twenty moorings were deployed over 22 months from 178.753W to 168.225W, with current meters at nominal depths of 2500, 4000, and 6000 m (or near-bottom where the bottom is shallower than 6000 m). Seven moorings west of 177W are located over the steep sides of the trench and the adjacent eastern flank of the Kermadec Island Arc. The axis of the observed mean currents in this region (weighted by record length), is near 27°T . The isobaths, for both the trench and the island-arc eastern flank, have roughly the same orientation. Vertical profiles of the mean velocity rotated in this direction (Fig. 2) show a strong (exceeding 9 cm s^{-1}) positive (nominally equatorward) flow along isobaths banked against the island arc eastern flank. This feature is the core of the deep

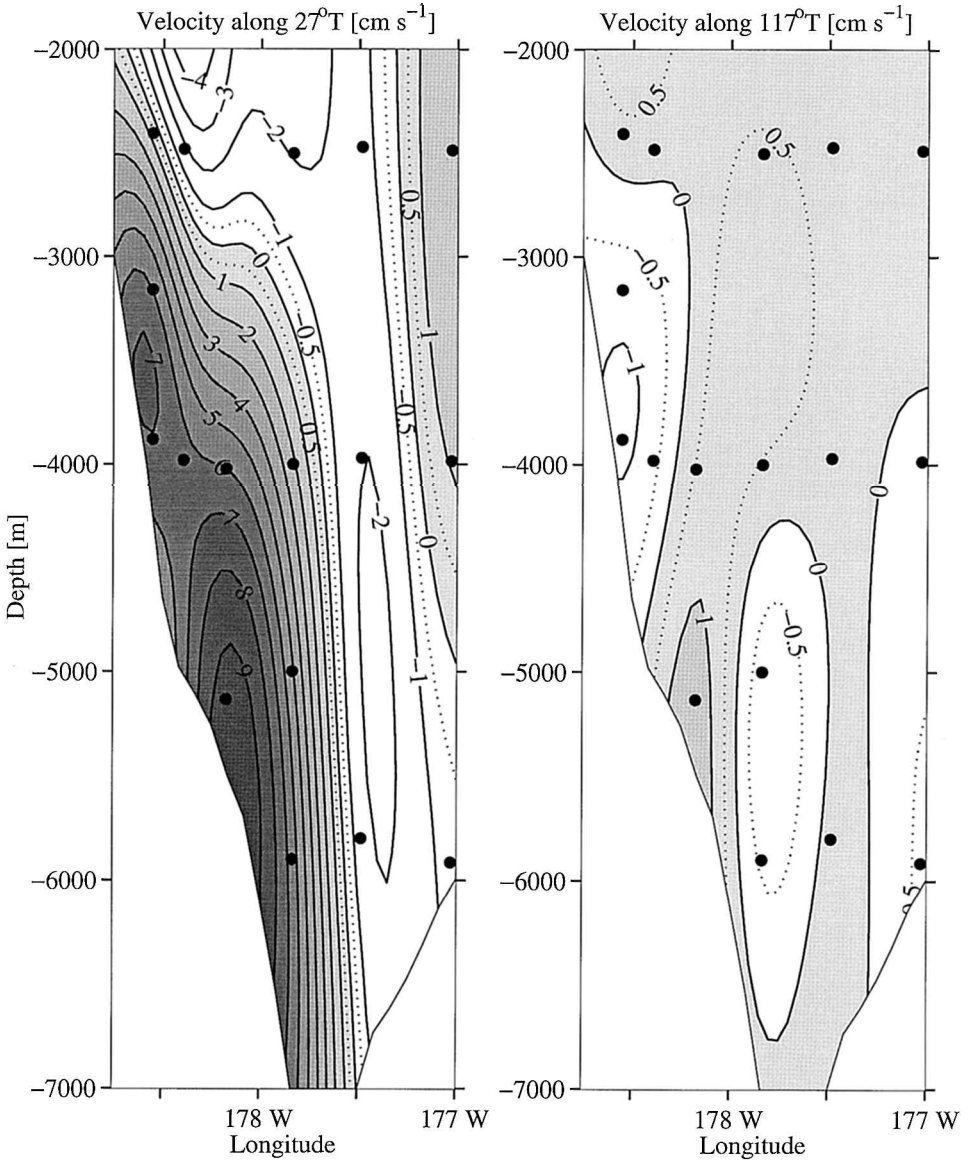


Figure 2. Vertical profiles of velocity components [cm s^{-1} , positive values shaded] parallel (left panel) and perpendicular (right panel) to the axis, 27°T , of mean velocity vectors over the Kermadec Trench from a current meter array along 32.5S (Whitworth *et al.*, 1996). The data are objectively mapped assuming a Gaussian covariance with correlation lengths of 1750 m in the vertical and 28 km in the horizontal and an error-to-signal energy of 0.01. The correlation lengths used are roughly the mean instrument spacings in the region and the error-to-signal energy is unrealistically low, so contours are faithful at and between current meters (black dots), but should be regarded with care outside array limits. Vertical exaggeration is 100:1. The 5-minute resolution ETOPO5 bathymetry is used. See Figure 5a for mooring locations and Figure 1 for trench location.

western-boundary current, consisting of Circumpolar Deep Water (Whitworth *et al.*, 1996). Offshore and shallower (around 2500 m), a weaker (exceeding 2 cm s^{-1}) negative (nominally poleward) return flow of Pacific Deep Water is found (Whitworth *et al.*, 1996). Most relevant to the point at hand, at deeper levels (4000 m and near-bottom) the flow remains nominally equatorward over the west side of the trench, but switches to a weaker (just exceeding 2 cm s^{-1}) negative (nominally poleward) flow over the east side of the trench. This pattern is consistent with the geostrophic velocities implied by the isotherm trough immediately over the trench (Whitworth *et al.*, 1996). The velocities perpendicular to the weighted mean current axis (Fig. 2) are everywhere small and less organized, as might be expected for the component roughly perpendicular to the isobaths.

Data are available from a small but useful current meter array at the southwest end of the Mariana Trench that also provide evidence for a cyclonic sense of circulation there. Statistics for these current meter records are available on the World-Wide-Web home page for the Division of Physical Oceanography in the Ocean Research Institute at the University of Tokyo (<http://dpo.ori.u-tokyo.ac.jp:81/>). Three current meter moorings, each with two current meters, were deployed across the southwest end of the trench. Here the trench axis is oriented roughly east-west, and the mooring line crosses it nominally along 142.6E (see Fig. 5b for mooring locations). Deployments started in July 1995 with record lengths from 370 to 441 days, and an average length of 424 days. Mooring latitudes range from 10.998 to 11.600N and instrument depths range from 6095 to 9860 m. The (record length weighted) mean velocity vectors for both current meters at each mooring are very closely aligned with the isobaths, and again the flow (not shown) is cyclonic in sense around the trench axis. On the north side of the trench, over the 6960-m isobath, the flow is nominally westward with a magnitude of 1.3 cm s^{-1} . At the center of the trench, over the 10286-m isobath, the velocity magnitude is a minimum at 0.1 cm s^{-1} . On the south side of the trench, over the 6520-m isobath, the flow is nominally eastward with a magnitude of 0.5 cm s^{-1} .

The next useful current meter array is at the north end of the Izu-Ogasawara Trench. These velocity data provide excellent evidence of the cyclonic sense of deep circulation over the trench. Again, statistics are available at <http://dpo.ori.u-tokyo.ac.jp:81/>. The focus here is on 30 current meter records nominally along 34N, longer than 100 days, with deployments starting as early as November 1987 and as late as May 1995. The record lengths range from 266 to 536 days, with an average of 401 days. Their longitudes range from 141.170 to 142.547E and their depths range from 3830 to 8961 m. The bathymetry here is more complicated than at the array over the Kermadec Trench, with a less uniform orientation of the trench walls. However, the moorings are roughly clustered at six locations, and the deep velocities are similar for most depths and deployments at each location. Therefore, the (record-length weighted) mean velocity vectors at each location are simply presented over the bathymetry (Fig. 3). The mean directions are very closely aligned with the isobaths, and again the sense of circulation is cyclonic around the trench axis. On the west side of the trench the flow is nominally equatorward with magnitudes of

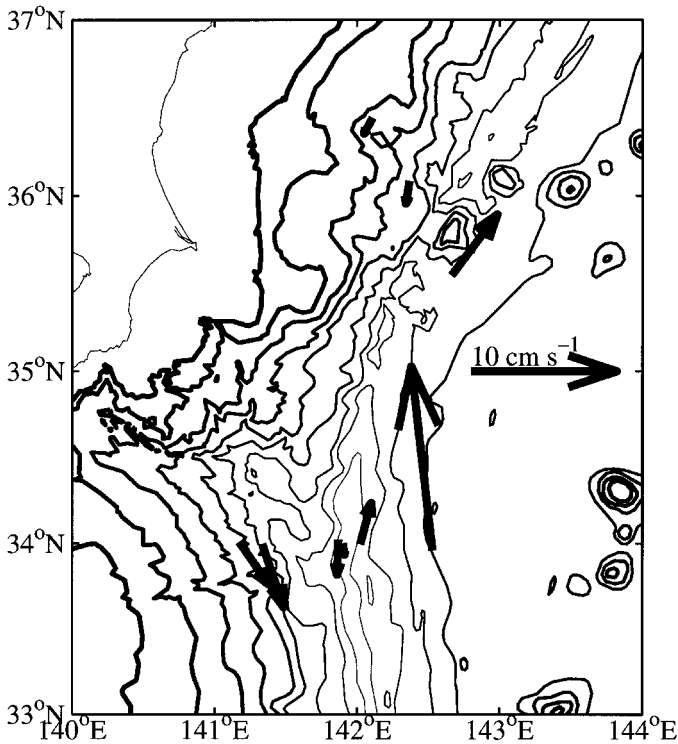


Figure 3. Mean deep current vectors over GEBCO bathymetry (IOC, IHO, and BODC, 1994). The Japan coast (thin lines), and isobaths at 1-km intervals (thickest line at 1 km to thinnest line at 9 km) are shown. Data from moorings along 34N (available on the World-Wide-Web home page for the Division of Physical Oceanography in the Ocean Research Institute at the University of Tokyo, <http://dpo.ori.u-tokyo.ac.jp:81/>) near the north end of the Izu-Ogasawara Trench are records exceeding 100 days. All are below 3800 m. Data near 36N (Hallock and Teague, 1996) are between 2000 and 4200 m at the south end of the Japan Trench. Vectors are averaged at each location (record length weighted) from instruments within these depth intervals. Data near 1900 and 4900 m at the eastern location near 36N are excluded for reasons discussed in the text, so the vector there is representative of 2900 m only. See Figure 5c for average mooring locations and Figure 1 for trench locations.

3.6, 4.6, and 2.4 cm s^{-1} , roughly over the 4500, 6000, and 9000-m isobaths, respectively. At the center of the trench the velocity magnitude is a minimum at 0.8 cm s^{-1} , nominally equatorward. On the east side of the trench the magnitude is 3.0 and 12.8 cm s^{-1} , but nominally poleward, roughly over the 9000 and 6000-m isobaths, respectively. A few more deep current meter records (again from <http://dpo.ori.u-tokyo.ac.jp:81/>) to the south (near 33 and 29N) also show nominally equatorward flow of similar magnitudes on the west side of the trench roughly over the 5000-m isobath, but these data are not shown here.

At around 36N is another deep current meter array at the western boundary spanning the Japan Trench near its southwestern end (Hallock and Teague, 1996) as well as RAFOS

floats deployed along the array at 3000 m. These data are mostly consistent with a cyclonic sense of deep circulation over the Japan Trench (Fig. 3). The current meter data have been used to document evidence of a weak, 1.3 and 1.6 cm s^{-1} , nominally equatorward, deep western-boundary current below 2000 m over the 3300 and 4600-m isobaths on the west side of the trench (Hallock and Teague, 1996). These authors have also summarized various other current meter records farther to the northeast at similar depths that show similar nominally equatorward velocities on the west side of the trench. The mean flow directions are all strongly aligned along isobaths, as in the previous examples. On the east side of the trench a stronger, 5.2 cm s^{-1} , nominally poleward flow exists near 2900 m over the 6400-m isobath (Hallock and Teague, 1996). Near 4900 m a relatively strong, 3.2 cm s^{-1} flow is found toward 318°T . This location is very close to Kashima 1 Guyot, which rises to around 3500 m, so the flow at 4900 m may be heavily influenced by this seamount and is not included in Figure 3. Measurements near 1900 m report an even stronger, 8.2 cm s^{-1} , nominally poleward, 65°T flow, in accord with expectations, but it may be sufficiently shallow to be unrepresentative of the abyss, so it is also not included in Figure 3. Neutrally buoyant RAFOS floats deployed at a nominal depth of 3000 m during current meter operations all show nominally poleward flow on the east side of the trench and, with the exception of the float deployed farthest west, weaker nominally equatorward flow on the west side of the trench (S. C. Riser, personal communication, 1997).

Deep current meter data over the Kuril Kamchatka Trench come from a recent deployment of nine moorings ranging in position along a line from 36.40N , 146.11E to 42.30N to 150.23E (W. B. Owens and B. A. Warren, personal communication, 1997). Yet again, the available current meter records are consistent with a deep cyclonic sense of circulation over the trench, with westward flow on its poleward side and eastward flow on its equatorward side. Current meters were deployed at nominal depths of 2000, 3000, and 4000 m for a length of 744 to 758 days, with one exception of a 379-day record. The northwestern mooring is located roughly over the 4000-m isobath on the poleward side of the trench axis. The magnitude of the mean velocity at 2000 and 3000 m is only 0.2 and 0.5 cm s^{-1} , but there is a 4.3 cm s^{-1} flow toward 259°T , nominally westward and roughly parallel to the isobaths, at 4000 m (see Fig. 5c for mooring locations). The next mooring to the southeast is located between the 7000 and 6500-m isobaths just on the equatorward side of the trench axis. This mooring has an extra instrument at a nominal depth of 5500 m and the exceptionally short record at 3000 m. The flow directions and magnitudes at this mooring are similar at all depths, and the record-length average is 8.1 cm s^{-1} toward 59°T , nominally eastward, again roughly parallel to the trench axis.

Finally, another current meter array was occupied over the Aleutian Trench along 175W (Warren and Owens, 1985; 1988). Since only two moorings are located over the trench, a cyclonic sense of circulation around the trench is only suggested by these data. This circulation may be shifted poleward of the trench axis because there is eastward flow over the axis. Five moorings were deployed over a fourteen-month period from 45.972 to 50.990N , with current meters at nominal depths of 2000, 3000, and 4500 m. The three

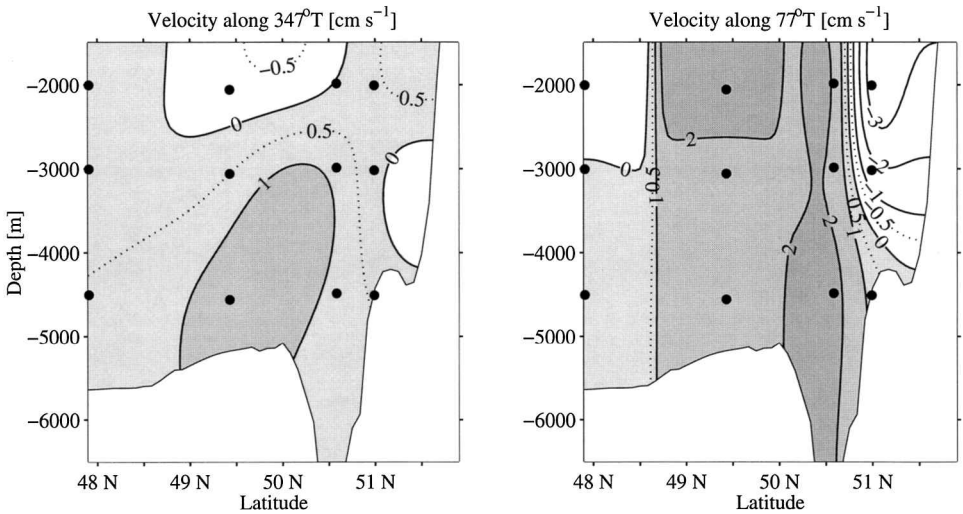


Figure 4. Vertical profiles of velocity components [cm s^{-1} , positive values shaded] oriented perpendicular (left panel) and parallel (right panel) to the axis, 77°T , of the mean velocity vectors over the Aleutian Trench from a deep current meter array along 175°W (Warren and Owens, 1985; 1988). The data are objectively mapped assuming a Gaussian covariance with correlation lengths of 1250 m in the vertical and 145 km in the horizontal and an error-to-signal energy of 0.01. The correlation lengths used are roughly the mean instrument spacings in the region and the error-to-signal energy is unrealistically low, so contours are faithful at and between current meters (black dots), but should be regarded with care outside array limits. Vertical exaggeration is 100:1. The 5-minute resolution ETOPO5 bathymetry is used. See Figure 5d for mooring locations and Figure 1 for trench location.

moorings north of 49°N are located over the steep topography of the trench and the rise just to the south. The axis of the observed mean currents in this region (weighted by record length), is near 77°T . The isobaths, for both the trench and the rise just to the south, have roughly the same orientation. Vertical profiles of the mean velocity rotated in this direction (Fig. 4) show a moderate (exceeding 3 cm s^{-1}) negative, nominally westward, flow along isobaths on the poleward side of the trench, banked against the Aleutian Island Arc. This flow is the expected deep northern-boundary current (Warren and Owens, 1985; 1988). Over the trench and on its equatorward flank is a slightly weaker (exceeding 2 cm s^{-1}) positive, nominally eastward, return deep flow previously without interpretation (Warren and Owens, 1985; 1988). The velocities perpendicular to the mean current axis (Fig. 4) are again everywhere small and less organized, as might be expected for the component roughly perpendicular to the isobaths.

In summary, available velocity measurements from long-term deep current meters and floats over the Kermadec, Mariana, Izu-Ogasawara, Japan, Kuril Kamchatka, and Aleutian Trenches are nearly all consistent with cyclonic gyres of at least a few cm s^{-1} magnitude around the trenches. These direct measurements are consistent with the inferences about the velocity field from hydrographic property distributions and geostrophic shear in the

studies reviewed in the previous section. The measurements interpreted here to imply cyclonic gyres above the trenches could also imply unconnected current-counter current pairs aligned with the trench axes, but the theoretical framework advanced below argues against this possibility.

4. Theoretical framework

For all of the trenches discussed in the previous two sections, the bathymetry unambiguously results in regions of closed planetary geostrophic, or f/h , contours. Here f is the local Coriolis parameter and h is the total thickness of the water column. Regional plots presented for the Kermadec and Tonga Trenches (Fig. 5a); the southern portion of the Mariana Trench (Fig. 5b); the Izu-Ogasawara, Japan, and Kuril Kamchatka Trenches (Fig. 5c); and the Aleutian Trench (Fig. 5d) confirm this assertion (see Fig. 1 for Fig. 5 panel locations). In some studies h is defined as the thickness of some deep layer beneath an arbitrary isobath or isopycnal (Kawase and Straub, 1991; Kawase, 1993a,b). Defining h as the total water-column thickness is a more stringent test for closed geostrophic contours. If a thinner abyssal layer alone were to feel the influence of the isobaths, the regions of closed contours over the trenches would be larger than those shown. At any rate, linearized planetary geostrophic theory requires blocked geostrophic contours, so it is not applicable where contours are closed. Hence, the trenches are special dynamical regions, as discussed below.

Numerical simulations of finite-depth abyssal layers under infinitely deep resting surface layers have shown that over regions with closed geostrophic contours upwelling results directly in vortex stretching that drives a cyclonic recirculation around these contours (Straub and Rhines, 1990; Kawase and Straub, 1991; Kawase, 1993a,b). Unlike eddy-driven flows, which have a direction dependent on the contour gradient, these recirculations are cyclonic in sense over both hills and trenches that result in regions of closed geostrophic contours, since they are driven by upwelling-induced vortex stretching. These experiments cannot reach a steady state because they rely on prescribed upwelling or a supply of mass to the abyssal layer for forcing and do not include vertical mixing. However, the abyssal upwelling or mass source can be kept small so the net abyssal layer thickness changes very slowly. The vortex stretching interior to a given closed geostrophic contour owing to the upwelling is balanced by the bottom drag along that contour, so the velocities within the regions of closed geostrophic contours reach a nearly steady balance.

For a similar dynamic balance to hold over the trenches, the mechanics must be along the following lines: A net upwelling over the trench is balanced by vertical diffusion at the top of the abyss. This upwelling maintains relatively low pressure just over the trench. In the abyss, where stratification is weak and flow nearly barotropic, conservation of potential vorticity tends to prevent water from flowing across geostrophic contours and eliminating the pressure gradient, so water recirculates cyclonically around the trench in geostrophic balance. Restated, the upwelling results in vortex stretching, driving a cyclonic recirculation around the trench. Water can cross geostrophic contours in a bottom Ekman layer or

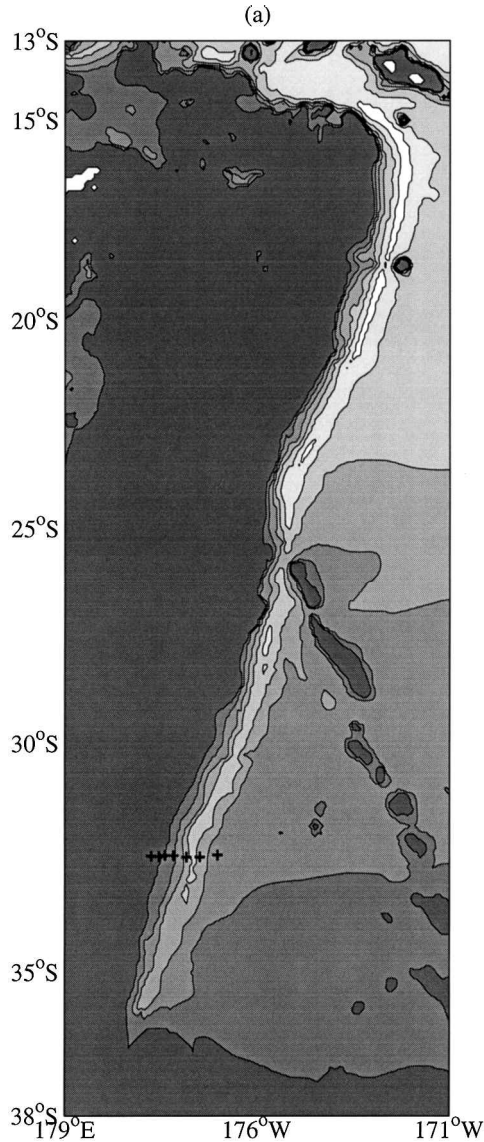


Figure 5. Absolute magnitude of planetary geostrophic, or f/h , contours [at $2 \times 10^{-9} \text{ m}^{-1} \text{ s}^{-1}$ intervals] where f is the local Coriolis parameter and h the total water depth, plotted for three different trench systems, (a) the Kermadec and Tonga Trenches [from 0.6 to $1.6 \times 10^{-8} \text{ m}^{-1} \text{ s}^{-1}$] with mooring locations for Figure 1 (+’s); (b) the southern portion of the Mariana Trench [from 0.2 to $1.2 \times 10^{-8} \text{ m}^{-1} \text{ s}^{-1}$] with the three mooring locations (+’s); (c) the Izu-Ogasawara, Japan, and Kuril Kamchatka Trenches [from 0.8 to $1.8 \times 10^{-8} \text{ m}^{-1} \text{ s}^{-1}$] with average locations for Figure 3 and the two moorings over the Kuril Kamchatka Trench (+’s); and (d) the Aleutian Trench with mooring locations for Figure 4 (+’s) [from 1.6 to $2.6 \times 10^{-8} \text{ m}^{-1} \text{ s}^{-1}$]. The 5-minute resolution ETOPO5 bathymetry is used. Some of the contours over each trench (lightest regions) are closed. The white regions are land masses. See Figure 1 for location of each panel.

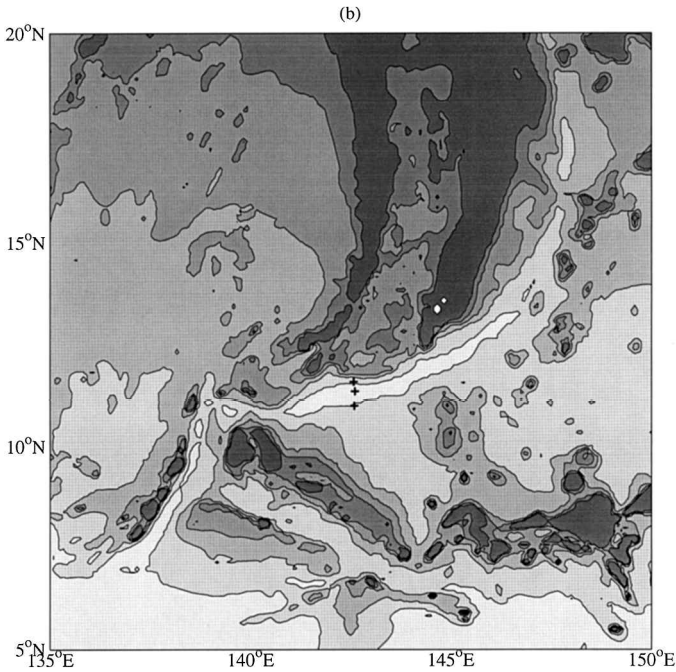


Fig. 5. (Continued)

where small-scale topographic relief allows ageostrophic flow, so the cyclonic recirculation is sufficiently strong such that the bottom ageostrophic transport into the trench balances the mass lost to upwelling. Restated, the magnitude of the upwelling-driven cyclonic recirculation is limited by bottom drag. After ventilating the trench ageostrophically near the bottom, water slowly spirals upward as it upwells and recirculates cyclonically around the trench.

More insight into the dynamical balance can be obtained by manipulating reduced-gravity, f -plane, shallow-water equations for an abyssal layer. In addition to the geostrophic balance, the momentum equation includes time-dependence, advection and a simple Rayleigh term, $R = (2\nu f)^{1/2} h^{-1}$, that multiplies the horizontal velocity \mathbf{u} . This term parameterizes friction as a bottom drag resulting from interior spin-down by vertical velocity at the top of the bottom Ekman layer. Here vertical eddy viscosity is ν , the Coriolis parameter is f , and the abyssal layer thickness is h . The continuity equation is fully nonlinear, retaining time-dependence and including a source term w with the dimensions of velocity to represent upwelling at the top of the abyss. Manipulation of the momentum and continuity equation gives a potential vorticity equation

$$q_t + \mathbf{u} \cdot \nabla q = q \frac{w}{h} - R \frac{\zeta}{h}, \quad (1)$$

where the potential vorticity $q = (f + \zeta)/h$, and the relative vorticity $\zeta = \nabla \times \mathbf{u}$.

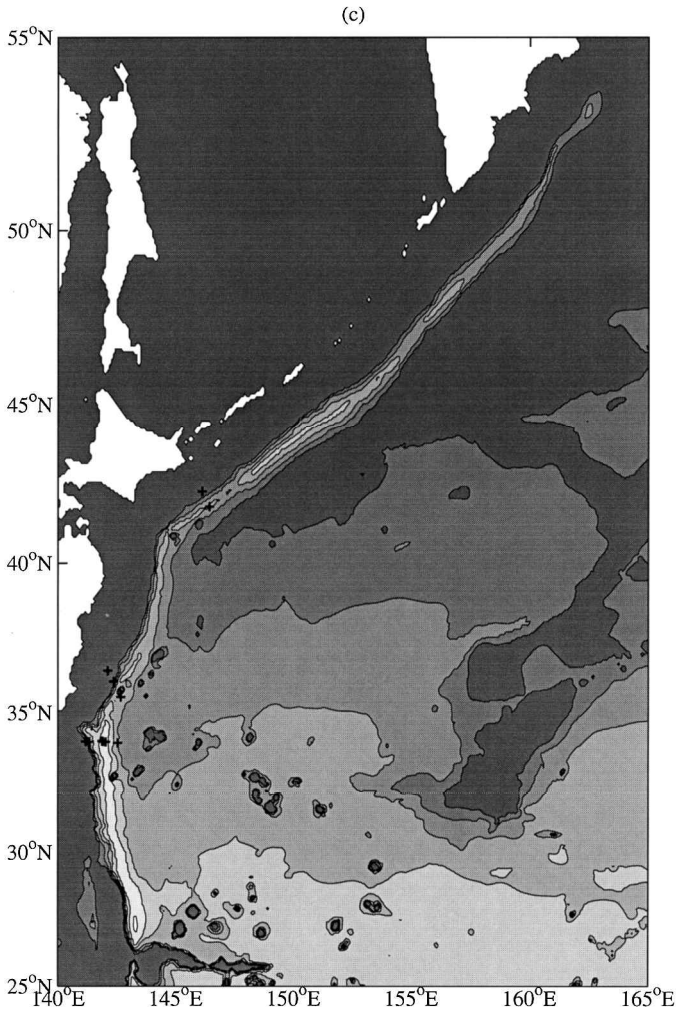


Fig. 5. (Continued)

Following Pedlosky (1987), a simple balance is obtained by multiplication of (1) by h followed by integration over a region, A_ψ , bounded by a closed geostrophic contour, C_ψ ,

$$\iint_{A_\psi} f \frac{w}{h} dA = \oint_{C_\psi} Ru \cdot dl. \tag{2}$$

The area integral of the upwelling drives vortex stretching that is balanced by bottom drag on circulation around the closed geostrophic contour. In deriving (2) upwelling is assumed to be balanced by vertical diffusion, so that the system is in steady-state and the time-dependence vanishes. The vertical advective-diffusive balance at the top of the abyss

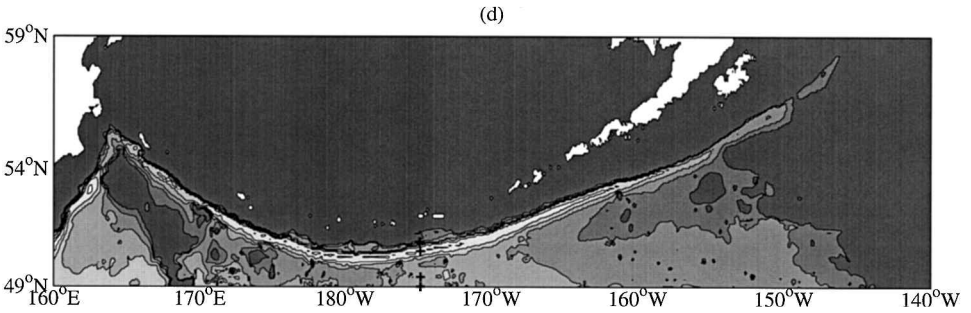


Fig. 5. (Continued)

coupled with the Ekman layer at the bottom allows application of the divergence theorem, so upon integration the advective term also vanishes. The upwelling term in (1) remains as an area integral in (2), with a simplification resulting from the assumption of small Rossby number so $\zeta \ll f$. The frictional curl term in (1) reduces to a line integral in (2) after integration and the application of Stoke's theorem.

This dynamical balance can be applied to the velocity data over the trenches to get an estimate of the magnitude of the necessary upwelling. For example, using the 5-minute resolution ETOPO5 bathymetry, the Izu-Ogasawara Trench is enclosed by $f/h = 1.15 \times 10^{-8} \text{ m}^{-1} \text{ s}^{-1}$, bounding an area of $7.2 \times 10^{10} \text{ m}^2$ (roughly 980 km in the meridional direction by 73 km in the zonal direction) with a path integral of length $2.3 \times 10^6 \text{ m}$. The deep velocity tangent to this geostrophic contour over the Izu-Ogasawara Trench is roughly 0.03 m s^{-1} . The area-averaged value of f/h inside this geostrophic contour is $0.99 \times 10^{-8} \text{ m}^{-1} \text{ s}^{-1}$; and the mean value of $(f)^{1/2}h^{-1}$ along the path is $1.3 \times 10^{-6} \text{ s}^{-1/2} \text{ m}^{-1}$. The least well constrained parameter is ν , which could conceivably range from 1×10^{-5} to $1 \times 10^{-2} \text{ m}^2 \text{ s}^{-1}$. Abyssal viscosity estimates are sorely lacking, so this range is based on a range for microstructure-based estimates of abyssal diffusion (Polzin *et al.*, 1997) assuming a Prandtl number between one and twenty. Fortunately, this parameter is under a square root, so the three-decade variability is reduced to a factor of thirty. These parameters yield upwelling velocities from 4.0×10^{-7} to $1.3 \times 10^{-5} \text{ m s}^{-1}$, a range roughly three to one hundred times one estimated interior value for the abyss (Stommel and Arons, 1960). While the present estimates are large, they fall well within the range of abyssal mass budgets for sill overflows, such as a recent one made north of the Samoan Passage (Roemmich *et al.*, 1996). The net volume transport of bottom water ageostrophically ventilating the trench required to feed the upwelling over it is reasonable. It ranges from 0.03×10^6 to $0.9 \times 10^6 \text{ m}^3 \text{ s}^{-1}$, at most a tenth of the net inflow of Circumpolar Deep Water into the North Pacific Ocean (Johnson and Toole, 1993). Were the effective vertical eddy viscosity and therefore the deep upwelling near the upper limits over most trenches, then a significant fraction of Circumpolar Deep Water could be cycled through these trenches as it moves around the Pacific Ocean.

5. Discussion

The observed deep cyclonic sense of circulation over the trenches is consistent with a theoretical framework predicting cyclonic recirculations driven by upwelling over regions of closed geostrophic contours. Of course, without other evidence, these recirculations could be driven by eddy potential-vorticity fluxes resulting from current meandering, waves, and other time-dependent phenomena in the upper ocean (Haidvogel and Rhines, 1983). In fact, the eddy driving does not have to occur over the entire trench, since such forcing over just a small region of the closed geostrophic contours has been shown to drive recirculation gyres (Thompson, 1995). Since most of the trenches discussed are overlaid somewhere by a near-surface boundary current or boundary current extension, this mechanism cannot be discounted as a potential driving mechanism for the cyclonic recirculations over the trenches. However, the relatively oxygen-rich and (in most locations) silica-poor character of water below the trench sills argues that the trenches must be relatively vigorously ventilated by bottom water, which must upwell over the trenches, most likely driving the cyclonic recirculations there.

This discussion of course begs the question of what forces the cyclonic recirculation. The simple vertical advective-diffusive balance posited for the deep ocean (Munk, 1966), where upwelling of cold water from below balances diffusion of heat from above, may dominate and allow a density gradient along the trench axis. Alternatively, the water at the trench bottom may be warmed mostly from below by geothermal heating, allowing it to upwell and be replaced by colder, denser, source water. The relative sizes of geothermal heating from below and vertical diffusion of heat out of the abyssal layer above the trench can be compared. There are few heat flow measurements within trenches, but the values around 0.050 W m^{-2} in the Japan Trench (Yamano and Uyeda, 1989) are similar to the 25 measurements characterized as being within Pacific Ocean trenches with depths greater than 5000 m reported by Pollack *et al.* (1993). The diffusive flux of heat from above is given by $\kappa \rho c_p \theta_z$, where $\rho c_p \sim 4 \times 10^6 \text{ J m}^{-3} \text{ }^\circ\text{C}$, and $\theta_z \sim 1 \times 10^{-4} \text{ }^\circ\text{C m}^{-1}$ for above the trench sills. For the two quantities to be of comparable magnitude requires a vertical diffusivity κ of $1 \times 10^{-4} \text{ m}^2 \text{ s}^{-1}$, certainly plausible for an abyssal value over steep topography (Polzin *et al.*, 1997). With the large uncertainty in κ and θ_z , it is difficult to speculate which effect might dominate.

Many long trenches exist, but no more of which we are aware have long-term velocity measurements over them. In the Pacific Ocean, the Philippine and Middle America Trenches are both significant trenches with closed geostrophic contours. These trenches are located in marginal basins, and may not have sufficient bottom water ventilation to drive a strong cyclonic recirculation. However, maps of bottom water properties including dissolved oxygen and silica do suggest that neither is totally stagnant (Mantyla and Reid, 1983). The Peru Chile Trench is probably long enough to be locally ventilated by bottom water at the southern end, supporting overall deep upwelling. This supposition is supported by a study of the abyssal flow in the region suggesting the Peru Chile trench is a primary

source of bottom water inflow for the Peru and Panama Basins (Lonsdale, 1976). The fact that this trench is adjacent to an eastern boundary may not have a large effect on the nature of the recirculation, except on how it is fed with dense water. However, the trench intersects the equator, meaning the geostrophic contours are not closed. Thus, there should only be a deflection of the normal planetary geostrophic flow warped by the topography, not nearly as strong as the cyclonic recirculations (Kawase, 1993a). In the Atlantic Ocean, a long trench that might have a cyclonic recirculation similar to those discussed previously is the South Sandwich Trench. In the Indian Ocean, the Java Trench, which intersects the equator and sits on an eastern boundary, is probably dynamically similar to the Peru Chile Trench in the Pacific Ocean.

It would be interesting to quantify the strengths of upwelling and recirculation around a deep trench. The recirculation strength in the trenches may dwarf the size of the net along-trench flow and upwelling, as suggested by the theoretical framework advanced in the previous section. In addition, the presence of deep western-boundary currents frequently confounds matters. These factors would make it difficult to sufficiently instrument a trench with current meters to diagnose the recirculation, net flow, and upwelling. Careful hydrographic measurements do reveal water-property contrasts and geothermal shear. However, the small signals, the potential for aliasing owing to the synoptic nature of the measurements, and the difficulty in determining reference velocities all mean that diagnosing an accurate absolute horizontal circulation much less upwelling over the trenches with hydrographic data alone is virtually impossible. Deep float measurements would be difficult because side walls present problems below trench sills and above trench sills the floats might wander away from the narrow trenches. One possibility for quantifying the net flow and upwelling strength is a deliberate tracer release experiment. The path length of closed geostrophic contours and the magnitude of the deep cyclonic velocity for the Izu-Ogasawara Trench (if the velocity measurements at the north end are typical) suggest an advective time-scale of two years for flow to cycle around the trench, a period that makes it amenable to such a technique. For the range of vertical velocity estimated in the discussion, a rise of between 30 and 1000 m would be expected in one circuit of the hypothesized spirals described by deep water parcels over the trench. The horizontal and vertical movement and spreading of a tracer patch released below the trench sill on one side of the trench could be used to diagnose the deep circulation and upwelling there.

Acknowledgments. This work was funded by the NOAA Office of Global Programs through the Climate and Global Change Program and the NASA Physical Oceanography Program. The work would not have been possible without the current meter and float data collected, some of it quite recently, and kindly provided prior to publication by Worth D. Nowlin, Jr., W. Brechner Owens, Stephen C. Riser, Keisuke Taira, Bruce A. Warren, and Thomas Whitworth, III. Their efforts are gratefully acknowledged. LuAnne Thompson helped with theoretical considerations. The comments of Bruce Warren and an anonymous referee greatly improved the manuscript. This is PMEL contribution number 1909.

REFERENCES

- Haidvogel, D. B. and P. B. Rhines. 1983. Waves and circulations driven by oscillatory winds in an idealized ocean basin. *Geophys. Astrophys. Fluid Dyn.*, *25*, 1–63.
- Hallock, Z. R. and W. J. Teague. 1996. Evidence for a North Pacific deep western boundary current. *J. Geophys. Res.*, *101*, 6617–6624.
- IOC, IHO and BODC. 1994. Supporting volume to the GEBCO Digital Atlas. Published on behalf of the Intergovernmental Oceanographic Commission (of Unesco) and the International Hydrographic Organization as part of the General Bathymetric Chart of the Oceans (GEBCO), British Oceanographic Data Centre, Birkenhead. This volume accompanies a CD-ROM.
- Johnson, G. C. and J. M. Toole. 1993. Flow of deep and bottom waters in the Pacific at 10°N. *Deep-Sea Res. I*, *40*, 371–394.
- Kawase, M. 1987. Establishment of deep ocean circulation driven by deep water production. *J. Phys. Oceanogr.*, *17*, 2294–2317.
- Kawase, M. 1993a. Effects of a concave bottom geometry on the upwelling-driven circulation in an abyssal ocean basin. *J. Phys. Oceanogr.*, *23*, 400–405.
- 1993b. Topographic effects on the bottom water circulation of the western tropical North Atlantic Ocean. *Deep-Sea Res. I*, *40*, 1259–1283.
- Kawase, M. and D. Straub. 1991. Spinup of source-driven circulation in an abyssal basin in the presence of bottom topography. *J. Phys. Oceanogr.*, *21*, 1501–1514.
- Kenyon, K. 1983. Sections along 35°N in the Pacific. *Deep-Sea Res.*, *30*, 349–369.
- Lonsdale, P. 1976. Abyssal circulation of the southeastern Pacific and some geological implications. *J. Geophys. Res.*, *81*, 1163–1176.
- Mantyla, A. W. and J. L. Reid. 1983. Abyssal characteristics of the World Ocean waters. *Deep-Sea Res.*, *30*, 805–833.
- Munk, W. 1966. Abyssal recipes. *Deep-Sea Res.*, *13*, 207–230.
- Pedlosky, J. 1987. *Geophysical Fluid Dynamics*, Springer Verlag, New York, 710 pp.
- Pollack, H. N., S. J. Hurter and J. R. Johnson. 1993. Heat flow from the Earth's interior: Analysis of the global data set. *Rev. Geophys.*, *31*, 267–280.
- Polzin, K. L., J. M. Toole, J. R. Ledwell and R. W. Schmitt. 1997. Spatial variability of turbulent mixing in the abyssal ocean. *Science*, *276*, 93–96.
- Rhines, P. B. and P. MacCready. 1989. Boundary control over the large-scale circulation. Proc. Fifth 'Aha Huliko'a Hawaiian Winter Workshop on Parameterization of Small-Scale Processes, Hawaii Institute of Geophysics, Honolulu, 75–97.
- Roemmich, D., S. Hautala and D. Rudnick. 1996. Northward abyssal transport through the Samoan passage and adjacent regions. *J. Geophys. Res.*, *101*, 14093–14055.
- Roemmich, D., T. McCallister and J. Swift. 1991. A transpacific section along latitude 24°N: the distribution of properties in the subtropical gyre. *Deep-Sea Res.*, *1*, 38, Suppl. 1, S1–S20.
- Speer, K. G. and M. McCartney. 1992. Bottom water circulation in the western North Atlantic. *J. Phys. Oceanogr.*, *22*, 83–92.
- Speer, K. G., G. Seidler and L. Talley. 1995. The Namib Col Current. *Deep-Sea Res. I*, *42*, 1933–1950.
- Stommel, H. and A. B. Arons. 1960. On the abyssal circulation of the World Ocean—II. An idealized model of the circulation amplitude and pattern in oceanic basins. *Deep-Sea Res.*, *6*, 140–154.
- Straub, D. N. and P. B. Rhines. 1990. Effects of large-scale topography on abyssal circulation. *J. Mar. Res.*, *48*, 223–253.
- Talley, L. D. and T. Joyce. 1992. The double silica maximum in the North Pacific. *J. Geophys. Res.*, *97*, 5465–5480.

- Talley, L. D., T. M. Joyce and R. A. DeSzoek. 1991. Transpacific section at 47°N and 152°W: distribution of properties. *Deep-Sea Res. I*, 38, Suppl. 1, S63–S82.
- Thompson, L. 1995. The effect of continental rises on the wind-driven ocean circulation. *J. Phys. Oceanogr.*, 25, 1296–1316.
- Warren, B. A. 1973. Transpacific hydrographic sections at Lats 43°S and 28°S; the SCORPIO Expedition-II. Deep water. *Deep-Sea Res.*, 20, 9–38.
- 1981. Deep circulation of the World Ocean, in *Evolution of Physical Oceanography, Scientific Surveys in Honor of Henry Stommel*, B. A. Warren and C. Wunsch, eds., The MIT Press, Cambridge, Massachusetts, 6–41.
- 1982. The deep water of the Central Indian Basin. *J. Mar. Res.*, 40, Suppl., 823–860.
- Warren, B. A. and W. B. Owens. 1985. Some preliminary results concerning deep northern-boundary currents in the North Pacific. *Prog. Oceanogr.*, 14, 537–551.
- 1988. Deep currents in the central subarctic Pacific Ocean. *J. Phys. Oceanogr.*, 18, 529–551.
- Warren, B. A. and K. G. Speer. 1991. Deep circulation in the Eastern South Atlantic Ocean. *Deep-Sea Res.*, 38, Suppl., S281–S322.
- Welander, P. 1969. Effects of planetary topography on the deep-sea circulation. *Deep-Sea Res.*, 16, Suppl., 369–392.
- Whitworth, T., III, B. A. Warren, W. D. Nowlin, Jr., S. B. Rutz, R. D. Pillsbury and M. I. Moore. 1996. On the deep western-boundary current in the Southwest Pacific Ocean, *Prog. Oceanogr.*, (submitted).
- Yamano, M. and S. Uyeda. 1989. Heat flow in the western Pacific, *CRC Handbook of Seafloor Heat Flow*, J. A. Wright, K. E. Loudon and J. R. Moore, eds., CRC Press, Inc., Boca Raton, Florida, 277–303.